Redox Biology 12 (2017) 103–113

Contents lists available at ScienceDirect

Redox Biology

journal homepage: www.elsevier.com/locate/redox

Research Paper

Influence of oxygen partial pressure on the characteristics of human hepatocarcinoma cells

Jenifer Trepiana, Susana Meijide, Rosaura Navarro, M. Luisa Hernández, José Ignacio Ruiz-Sanz*, M. Begoña Ruiz-Larrea*

Department of Physiology, Medicine and Nursing School, University of the Basque Country UPV/EHU, 48940 Leioa, Spain

ARTICLE INFO

Keywords:
Oxygen tension
Hepatoma cells
Superoxide dismutase
Cell migration

ABSTRACT

Most of the *in vitro* studies using liver cell lines have been performed under atmospheric oxygen partial pressure (21% O_2). However, the oxygen concentrations in the liver and cancer cells are far from this value. In the present study, we have evaluated the influence of oxygen on 1) the tumor cell lines features (growth, steady-state ROS levels, GSH content, activities of antioxidant enzymes, p66 Shc and SOD expressions, metalloproteinases secretion, migration, invasion, and adhesion) of human hepatocellular carcinoma cell lines, and b) the response of the cells to an oxidant stimulus (aqueous leaf extract of the *V. baccifera* plant species). For this purpose, three hepatocarcinoma cell lines with different p53 status, HepG2 (wild-type), Huh7 (mutated), and Hep3B (deleted), were cultured (6–30 days) under atmospheric (21%) and more physiological (8%) pO_2. Results showed that after long-term culturing at 8% *versus* 21% O_2, the cellular proliferation rate and the steady-state levels of mitochondrial O_2^- were unaffected. However, the intracellular basal ROS levels were higher independently of the characteristics of the cell line. Moreover, the lower pO_2 was associated with lower glutathione content, the induction of p66 Shc and Mn-SOD proteins, and increased SOD activity only in HepG2. This cell line also showed a higher migration rate, secretion of active metalloproteinases, and a faster invasion. HepG2 cells were more resistant to the oxidative stress induced by *V. baccifera*. Results suggest that the long-term culturing of human hepatoma cells at a low, more physiological pO_2 induces antioxidant adaptations that could be mediated by p53, and may alter the cellular response to a subsequent oxidant challenge. Data support the necessity of validating outcomes from studies performed with hepatoma cell cultures under ambient O_2.

1. Introduction

In physiological conditions, oxygen supply and diffusion into tissues are necessary for survival. The oxygen partial pressure results from the balance between oxygen delivery into an organ and its consumption. Although the pO_2 at ambient atmosphere is equivalent to 21%, tissue oxygenation progressively decreases as it reaches internal organs and tissues [1]. The level of O_2 and its distribution among the various tissues depends on the rate of capillary blood flow and the tissue metabolic activity. Consequently, in humans under physiological conditions, the pO_2 in well-irrigated organs such as lungs, liver and kidneys, ranges from 4% to 14% [2,3]. The oxygen concentration in tumor cells is heterogeneous and depends on the distance of the cell from the blood vasculature. Cells that reside far away from blood vessels can even become hypoxic, receiving inadequate amounts of oxygen [4]. Most of the *in vitro* experiments using cell cultures are typically performed in atmospheric O_2 levels (21%), thus, in a non-physiological environment. An inadequate (absent or in excess) oxygen tension in cell cultures can result in the production of reactive oxygen species (ROS) and the induction of oxidative stress [5–7], with consequences on the cellular behaviour leading to cell growth or death [8]. The change in the redox status of the cell may alter the expression of antioxidant enzymes, cell proliferation, migration and invasion [8,9]. Oxygen finely regulates cell activity from the gene level to the proteome expression [10]. It has been reported that the long-term culturing of transformed human and murine myeloid cell lines under atmospheric oxygen levels (21% O_2) or more physiological pO_2 (5% O_2) induced significant differential phenotype changes in free surface thiol expression, total GSH content, and sensitivity to hydrogen peroxide [11].

The p53 tumor suppressor protein plays key roles in regulating cell-cycle and apoptosis. The protein regulates the expression of various mitochondrial-targeted genes that affect pro-apoptotic proteins, leading to cell death [12]. p53 also possesses potent redox-regulating activity through modulating various ROS-generating and antioxidant

* Corresponding authors.
E-mail addresses: joseignacio.ruizs@ehu.eus (J.I. Ruiz-Sanz), mbego.ruizlarrea@ehu.eus (M.B. Ruiz-Larrea).

http://dx.doi.org/10.1016/j.redox.2017.02.004
Received 14 December 2016; Received in revised form 24 January 2017; Accepted 7 February 2017
Available online 13 February 2017
2213-2317/ © 2017 The Authors. Published by Elsevier B.V.
This is an open access article under the CC BY-NC-ND license (http://creativecommons.org/licenses/BY-NC-ND/4.0/).

enzymes, particularly p66 Shc and MnSOD [13,14]. p66 Shc has recently emerged as a redox sensor that transmits oxidative stress signals to DNA damage in hepatocytes [15]. Activated p66 Shc is localized in mitochondria, where the molecule generates hydrogen peroxide to initiate the apoptotic cascade [16,17].

In a previous work, we described that an aqueous leaf extract of the Amazonian *V. baccifera* plant species induced intracellular accumulation of ROS and toxicity to several human hepatocellular carcinoma cell lines cultured under atmospheric O_2. Results suggested that oxidative stress was involved in cell death [18]. In the present study, we have evaluated the influence of the oxygen partial pressure on 1) the tumor features (growth, steady-state ROS levels, GSH content, activities of antioxidant enzymes, p66 Shc and SOD expressions, migration, invasion, metalloproteinases secretion, and adhesion) of human hepatocellular carcinoma cell lines, and b) the response of the cells to an oxidant stimulus (*V. baccifera* leaf extract). For this purpose, three hepatocarcinoma cell lines with different p53 status, HepG2, Huh7, and Hep3B, were long-term (6–30 days) cultured under atmospheric (21%) and more physiological (8%) pO_2. HepG2 cells carry wild-type p53, in Hep3B the p53 gene is deleted [19], and p53 expressed in Huh7 conserves around 4% wild type transactivating activity [20]. Data suggest that the long-term culturing of human hepatoma cells under low pO_2 induces antioxidant adaptations that may modify the cellular response to a subsequent oxidant challenge, and support the necessity of using low, more physiological oxygen tensions in culturing tumor cell lines to draw conclusions applied to cancer biology from *in vitro* studies.

2. Materials and methods

2.1. Reagents

Bis-(3-carboxy-4-nitrophenyl)-disulphide (DTNB), 3,4-dichloronitrobenzene (CDNB), glutathione, glutathione reductase, horseradish peroxidase (HRP), hydrogen peroxide, NADPH, nitro-blue tetrazolium (NBT), sulfosalicylic acid, trypsin, xanthine and xanthine oxidase (XOD) were all obtained from Sigma-Aldrich (St Louis, MO, USA). Anti-Cu,Zn-SOD antibody was purchased from Calbiochem (La Jolla, CA, USA), anti-Mn-SOD and anti-Shc antibodies from Millipore (Darmstadt, Germany), and Amersham ECL Western Blotting Detection Reagent from GE Healthcare (Chicago, Illinois, USA).

2.2. Culture and maintenance of cell lines

The human hepatoma cell lines HepG2, Huh7 and Hep3B were purchased from ATTC (American Type Culture Collection, Manassas, USA). These cells were maintained in Eagle's Minimum Essential Medium (EMEM) (ATCC) supplemented with 10% heat inactivated fetal bovine serum (FBS) (ATCC), 2 mM L-glutamine, 0.1 mg/ml streptomycin and 100 U/ml penicillin (all from Sigma-Aldrich, St Louis, MO, USA). Shortly after establishment of consistent cell lines in 75 cm^2 flasks under 21% pO_2 at 37 °C in humidified atmosphere with 5% CO_2, each cell line was divided into two flasks and cultured under similar conditions except for the O_2 concentration (21% and 8% pO_2). Cells were cultured in a Thermo Fisher Scientific HERAcell incubator (Waltham, MA, USA) equipped with two gas monitoring systems, CO_2 and O_2/N_2 (nitrogen to reduce the oxygen levels). All media were preequilibrated to the O_2 conditions in the incubator before their use. All cell passages were performed quickly in the laminar flow cabinet when the cell monolayer reached around 75% of confluence. Cells were detached with a solution of 0.1% trypsin-0.04% EDTA and then harvested to perform subsequent experimentations. Cells adapted to the pO_2 regimen for a minimum of six days and a maximum of 30 days before the corresponding experiment.

The Ethical Committee for Researching with Biological Agents (CEIAB) from the University of the Basque Country, UPV/EHU, approved the protocol (M30_2015_2013_RUIZ SANZ).

2.3. Plant aqueous extract

The aqueous leaf extract of *V. baccifera* was prepared from infusions, as has been described in Lizcano et al. [21].

2.4. Cell proliferation assay

Cells cultured under both pO_2 conditions described in point 2.2 were seeded onto 96-well plates and cultured under both different oxygen conditions and at different cell densities (2,000, 2,500 and 3,000 cells per well). Their growth was registered every 24 h for 5 days, following the crystal violet stain method according to Gillies et al. [22]. This consisted in removing medium, washing the cells once with phosphate buffered saline (PBS) and fixing them for 15 min with a 3.7% formaldehyde solution. Then, the cells were washed twice with PBS and stained with a 0.25% crystal violet solution (Merck, Darmstadt, Germany) for 20 min in the dark. After this, plates were washed with running water and when they were dry, 150 µl of a 33% acetic acid solution was added in each well to dissolve crystal violet.

The absorbance was measured at 590 nm in a Synergy HT microplate reader (BioTek, Winooski, VT, USA). Considering that absorbance is proportional to the cell density, the obtained data were represented as exponential growth curves. Duplication times were derived from semi-logarithm representations of the absorbance *versus* the culture time, and were calculated using the following formula: $A=A_0\times 2^{t/DT}$; *DT* refers to the duplication time; *t* to the culture time and A_0 and A refer to absorbances at zero and at any time, respectively.

2.5. Intracellular ROS and mitochondrial O_2^- detection

Intracellular ROS levels were measured using the cell-permeant 2′,7′-dichlorodihydrofluorescein diacetate (H_2DCF-DA) probe (Molecular Probes, Eugene, OR, USA), which is deacetylated and oxidized inside the cell producing the 2′,7′-dichlorofluorescein (DCF) fluorescent compound. Cells cultured under both pO_2 conditions described in point 2.2 were seeded at a density of 2.5×10^5 cell per well onto 6-well plates and maintained under the two oxygen concentrations for additional 48 h, and before treatment (addition of *V. baccifera* extract). After that, cells were washed, resuspended in the corresponding medium (8% and 21% O_2) and incubated with H_2DCF-DA (20 µM) for 30 min at 37 °C in the dark. Then the probe solution was removed and, after washing with PBS, the cells were trypsinized and harvested to analyze the DCF fluorescence of the live cells by flow cytometry in a Beckman Coulter Gallios Flow Cytometer (λ_{exc}=485/20 and λ_{em}=528/20) in the General Research Services SGIker of the UPV/EHU (http://www.ikerkuntza.ehu.es/p273-sgikerhm/en/). At least 10,000 cells (events) were detected for each group. Data obtained from flow cytometry were analyzed using Summit 4.3 software (Dako, Hovedstaden, Denmark). Intracellular ROS levels were expressed as the mean fluorescence signal (arbitrary units) of the analyzed live cell population (10,000 events).

The mitochondrial superoxide anion levels were measured using the cell-permeant MitoSOX™ Red reagent (Molecular Probes, Eugene, OR, USA), which is selectively targeted to mitochondria and oxidized by superoxide. Cells were incubated in the corresponding medium (8% and 21% O_2) with MitoSOX (4 µM) for 30 min at 37 °C in the dark. The fluorescence intensity from live cells was analyzed by flow cytometry in a Beckman Coulter Gallios Flow Cytometer (λ_{exc}=485/20 and λ_{em}=620/20) in the General Research Services SGIker of the UPV/EHU. Results were expressed as the mean fluorescence signal (arbitrary units) of the analyzed live cell population (10,000 events).

2.6. Determination of GSH

Cells cultured under both pO_2 conditions described in point 2.2 were seeded at a density of 1×10^6 cells onto Petri dishes and further maintained under both pO_2 conditions for 72 h. Cells were washed with ice-cold PBS and resuspended in ice-cold lysis buffer (0.1% Triton X-100% and 0.6% sulfosalicylic acid) and lysed by a freezing and thawing process. After that, cells were centrifuged at 4,000×*g* for 5 min at 4 °C and the supernatant was collected. The total protein was quantified in the supernatant.

The measurement of glutathione (GSH) was evaluated with the glutathione reductase-DTNB recycling method, as reported previously [23]. Reaction was run in 96-well microplates; 5 µl of each sample were distributed per well for quantification of total GSH. Glutathione reductase (1.82 Units/well), DTNB (458 µM) and NADPH (0.3 mM for GSH) were then added to a final volume of 220 µl/well. Absorbance was monitored at 412 nm. The GSH concentration was estimated from a standard curve. Results were expressed as nmol of GSH per mg of protein.

2.7. Immunodetection of proteins

Cu,Zn-superoxide dismutase (Cu,Zn-SOD), Mn-superoxide dismutase (Mn-SOD) and p66, p52 and p46 Shc isoforms were detected by immunoblotting. Cellular protein extracts were boiled at 95 °C for 5 min in Laemmli sample buffer (300 mM Tris-HCl, pH 6.8, 50% glycerol, 10% SDS, 250 mM DTT, 0.01% bromophenol blue) [24] and were separated by SDS-PAGE electrophoresis in 15% (Cu,Zn-SOD and Mn-SOD) or 10% (Shc) polyacrylamide gels. Gels were transferred onto PVDF membranes by electro-blotting with constant amperage (1 mA/cm^2). After blocking for 1 h at room temperature, membranes were incubated overnight at 4 °C with the corresponding primary antibody (anti-Cu,Zn-SOD 1:7000, anti-Mn-SOD 1:2000, and anti-Shc 1:2000). After washing, membranes were probed with its secondary antibody conjugated to horseradish peroxidase for 1 h at room temperature. The immunoreactive proteins were detected with an enhanced chemiluminescence (ECL) substrate kit (Amersham ECL Western Blotting Detection Reagent, GE Healthcare) and exposure to X-ray films. Bands were quantified by densitometry. Glucose-6-phosphate deydrogenase was used as loading control.

To characterize mass expression of SOD isoforms, a standard curve (6.6–33 ng Cu,Zn-SOD and 1.6–7.9 ng Mn-SOD) was prepared using commercial human recombinant SOD protein (ProSpec-Tany TechnoGene Ltd., Israel). Values were interpolated in the linear range of the standard curve. The amount of protein was expressed as ng/mg of protein.

2.8. Enzymatic assays

All cell types grown by long-term exposure to 21% O_2 and 8% O_2 tension were lysed by freeze-thaw in liquid N_2. Protein concentration was quantified [25] in the cell extract.

2.8.1. Superoxide dismutase activity (EC 1.15.1.1)

SOD activity was determined indirectly by the method of nitro-blue tetrazolium (NBT) [26]. This method uses the xanthine-xanthine oxidase system to generate superoxide anions. The superoxide anion reduces NBT, which is converted into NBT-diformazan. This reduced form is blue, and the absorbance is recorded at 570 nm in a spectrophotometer. In presence of SOD, O_2^- undergoes a dismutation into O_2 and H_2O_2, decreasing the NBT-diformazan formation. Hence, this competing assay yields to the indirect measurement of SOD activity.

The method was adapted to 96 well plates. Increasing amounts of cellular protein were assayed for each independent experiment and the absorbance was determined *versus* the incubation time. The reaction was started by the addition of NBT (60 µM) in a final volume of 250 µl.

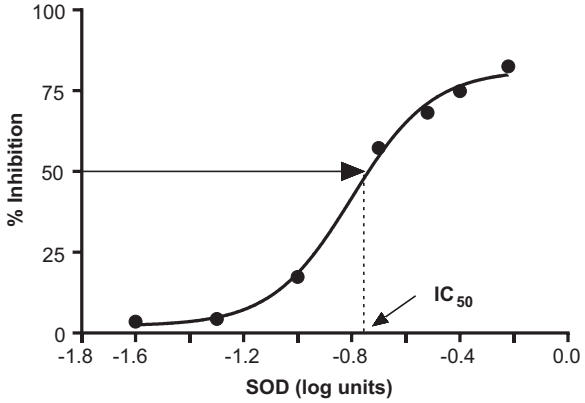

Fig. 1. Example of the inhibition curve built with commercial SOD to express the results as SOD units/mg of protein.

Table 1
Effect of pO_2 on growth of hepatocellular carcinoma cells.

	Doubling time (h)	
Cell type	21% pO_2	8% pO_2
HepG2	31.8 ± 0.9^a	29.1 ± 1.1^a
Huh7	32.1 ± 0.7^a	33.9 ± 0.5^b
Hep3B	26.4 ± 1.1^b	23.6 ± 0.9^c

Doubling times were derived from semi-logarithm representations of the crystal violet absorbance *versus* the incubation time. Results are expressed as the mean ± SE of 3–15 experiments. Data in the same column with different superscript are significantly different. $^{a,b,c}P < 0.05$.

The increase of absorbance was determined every 60 s for 12 min at a temperature of 37 °C. The slope of the curve for each protein concentration was calculated, and the percentage of inhibition relative to a control without protein was calculated. To calculate the IC_{50} (amount of protein required to inhibit the formation of NBT-diformazan by 50%) the % inhibition was plotted *versus* the log of protein concentration, and the graphs were adjusted to semi-logarithmic curves, using GraphPad Prism 4 for Windows (San Diego, CA, USA).

An inhibition curve was prepared using commercially available SOD (Sigma-Aldrich, St. Louis, MO, USA) to transform the IC_{50} value into SOD units (Fig. 1). Results are expressed as SOD U/mg of protein. One unit of SOD activity was defined as the amount of the enzyme in a sample solution causing 50% inhibition (IC_{50}) of the rate of reduction of tetrazolium salt [27].

2.8.2. Catalase (EC 1.11.1.6)

Catalase (CAT) activity was measured according to Aebi (1984) [28] by observing spectrophotometrically the H_2O_2 disappearance at 240 nm. The reaction took place in a final volume of 1 ml containing 90 mM potassium phosphate buffer (pH 6.8) and started with the addition of H_2O_2 (30 mM final concentration). Decrease in absorbance was continuously measured every 2 s over 1 min. CAT activity was expressed as µmol/min/mg of protein, using the experimental coefficient ε=0.04 mM^{-1}.

2.8.3. Glutathione peroxidase (EC 1.11.1.9)

Selenium-dependent glutathione peroxidase (GPx) activity was assayed by the indirect method of Flohé and Güntzler (1984) [29]. GPx activity was measured in a coupled enzyme system where NADPH is consumed by glutathione reductase (GR) to convert the formed glutathione disulphide (GSSG) to its reduced form (GSH). The decrease in absorbance of NADPH was monitored at 340 nm every 60 s for 15 min in a 96-well plate reader at 30 °C. The final volume was 225 µl containing 50 mM potassium phosphate buffer (pH 7.0), 1 mM EDTA-Na_2, 0.5 mM

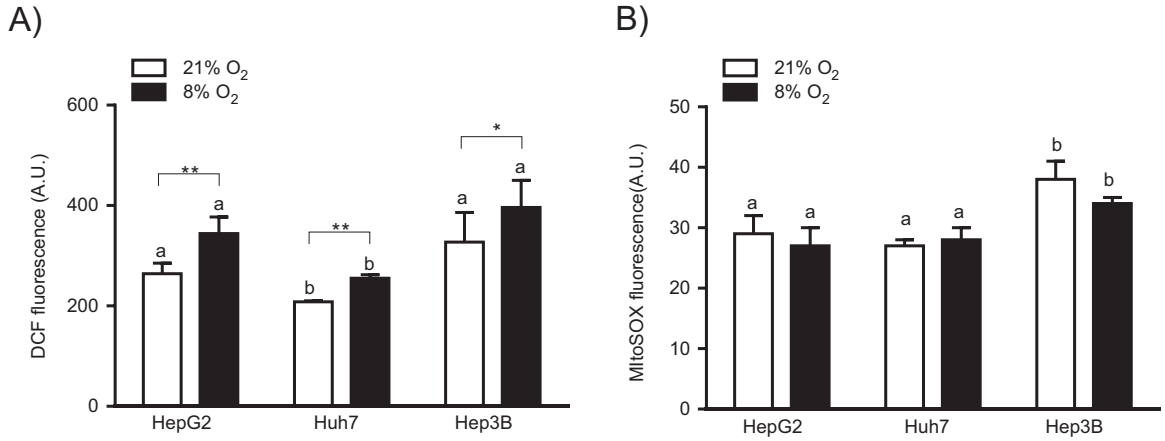

Fig. 2. Effect of pO_2 on (A) intracellular ROS and (B) mitochondrial O_2^- levels in hepatoma cell lines. Cells were incubated under 21% and 8% pO_2. The mean of DCF and MitoSOX fluorescences (arbitrary units) of the analyzed live cell population (10,000 events) is represented. Results are the mean+SE of 3–16 experiments. *P < 0.05, **P < 0.01, different between both pO_2 conditions in the same cell line. Bars with different superscript at the same pO_2 are significantly different, $^{a,b}P < 0.05$.

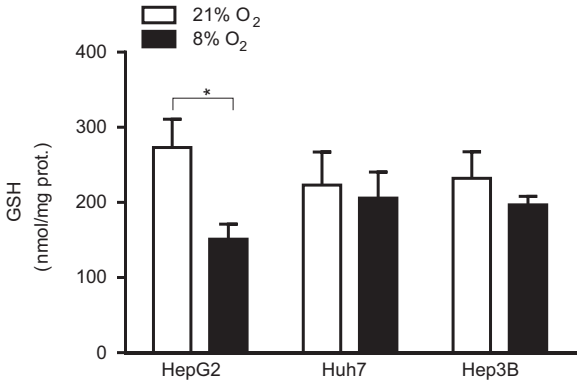

Fig. 3. Effect of pO_2 on the intracellular levels of GSH in hepatoma cell lines. Cells were incubated under 21% and 8% pO_2. Results are the mean+SE of 3–6 experiments. *P < 0.05 different between both pO_2 conditions in the same cell line.

sodium azide, 0.45 mM GSH, 0.2 mM NADPH and 0.45 U of GR. The reaction started by the addition of H_2O_2 (0.77 mM final concentration). The results are expressed as nmol/min/mg of protein, using the NADPH experimental coefficient ε=3.065 mM^{-1}.

2.8.4. Glutathione S-transferase (EC 2.5.1.18)

Glutathione S-transferase (GST) activity was assayed according to Habig and Jakoby (1981) [30], based on the conjugation of GSH with 3,4-dichloronitrobenzene (CDNB). The rate of GS-DNB appearance was monitored at 340 nm for 9 min in a 96-well microplate reader at 30 °C. The reaction mixture contained 78 mM potassium phosphate buffer (pH 6.5), 1 mM EDTA-Na_2, and 2 mM GSH in a total volume of 250 µl. The reaction started by the addition of CDNB (2 mM final concentration). The results are expressed as nmol/min/mg of protein, using the experimental coefficient ε=9.6 mM^{-1}.

2.9. Determination of total proteins

Total protein was quantified spectrophotometrically at 595 nm by Coomassie Brilliant Blue dying [25], using bovine serum albumin as standard.

2.10. Transwell migration and invasion assay

The migration ability of cells was carried out using 24-well transwell migration chambers (Greiner Bio-One, Switzerland) with 8 µm pore size polyethylene membranes. For cell invasion assay, transwell inserts were precoated with 68 µl of 5 µg/ml fibronectin (Sigma-Aldrich, St Louis, MO, USA) at 37 °C for 1 h for gelling. The upper chambers were inoculated with 6×10^4 cells/well in 0.2 ml serum-free EMEM solution. Lower chambers were filled with 0.6 ml of the corresponding medium containing the chemoattractant (10% FBS) and cells were allowed to migrate for 24 h under 21% pO_2 or 8% pO_2, at 37 °C in humidified atmosphere with 5% CO_2. After the incubation, cells located upon the upper membranes were wiped with cotton swabs. The cells that migrated to the lower surface of the polyethylene membranes were fixed in 70% ethanol overnight. Subsequently, cells were stained overnight with 25 µg/ml propidium iodide (Sigma-Aldrich, St Louis, MO, USA) and 200 µg/ml RNase A (Roche Biochemicals, Indianapolis, IN, USA). The inserts were photographed under an Olympus Fluoview FV500 confocal microscope in the General Research Services SGIker of the UPV/EHU (http://www.ikerkuntza.ehu.es/p273-sgikerhm/en/). The number of migrated and invasive cells was calculated using the ImageJ software (NIH, Bethesda, Maryland, USA).

2.11. Matrix metalloproteinase (MMP) activity determination by zymography

MMP activity was determined by zymography. This technique is used for chromatographic detection of proteinases in polyacrylamide gels. Gels are enriched with a protein substrate for the enzymatic activity to be detected. When the gels are stained with Coomassie Brilliant Blue, no stained bands are shown due to the substrate protein degradation by the proteinases [31].

Gelatin zymography was used to detect gelatinases activity. For the gelatin zymography, the samples (concentration conditioned medium) were mixed with non-reducing Laemmli buffer [24]. The resolving gel was 10% polyacrylamide with 0.1% gelatin in 390 mM Tris/HCl pH 8.8, 0.1% SDS buffer, and the stacking gel was 4% polyacrylamide in 65 mM Tris/HCl, 0.1% SDS buffer, pH 6.8. Gels were loaded with similar quantities of media and cellular protein. Each gel was loaded with pairs of cell line samples at 21% O_2 and 8% O_2. Commercial protein ladder for molecular weight identification were included in all zymographies. After running at 150 v for 75 min in electrophoresis buffer (25 mM Tris/HCl, 192 mM glycine and SDS 0.1%), gels were washed twice with a 2% Triton X-100 solution for 20 min, and immersed overnight at 37 °C in MMP substrate buffer (50 mM Tris/HCl, 10 mM $CaCl_2$, 3 mM NaN_3, pH 7.5). After washing with H_2O, gels were stained for 20 min (40% methanol, 10% acetic acid, and 0.1% Coomassie brilliant blue R-250). Gels were immersed in destaining solution (20% methanol, 10% acetic acid) until the bands were visible. Gels were digitalized with a densitometry image system (Molecular imager FX) and bands quantified with the Quantity One software (BioRad Laboratories, Inc).

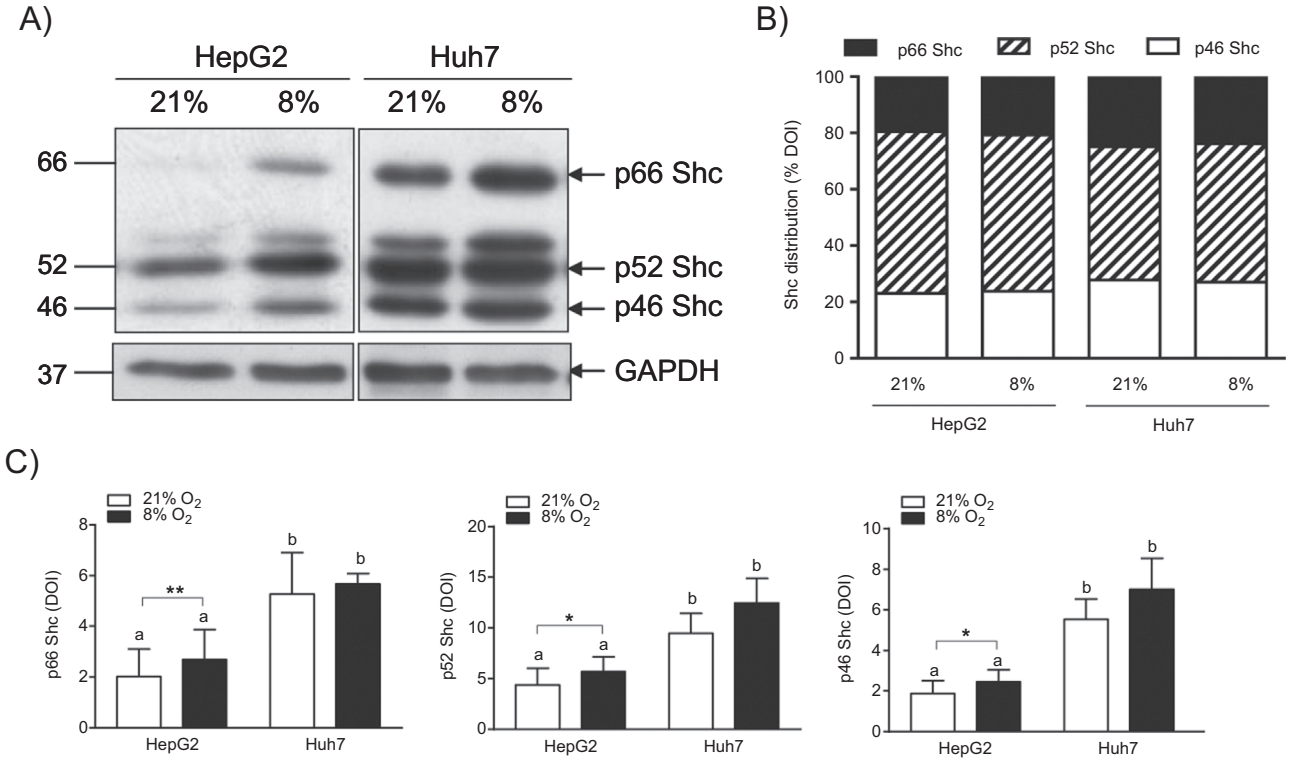

Fig. 4. Effect of pO_2 on p66, p52, and p46 Shc isoforms. HepG2 and Huh7 were incubated under 21% and 8% pO_2. (A) Proteins from cell extracts were analyzed by western blot. The bands shown are representative of 6 experiments. (B) Distribution of Shc proteins (as % of total DOI) under 21% and 8% pO_2. Data are the mean of 6 experiments. (C) Representation of the densitometry changes from the western blot results represented in (A). Results are the mean+SE of 6 experiments. *P < 0.05, **P < 0.01, different between both pO_2 conditions in the same cell line. Bars with different superscript at the same pO_2 are significantly different, $^{a,b}P < 0.05$.

2.12. Adhesion assay

Cells cultured under the conditions described in point 2.2 were seeded onto 96-well plates at 20,000 cells per well and further incubated for 1 h under 21% pO_2 and 8% pO_2. The cell adhesion was determined by the crystal violet stain method [22]. The number of adherent cells was calculated interpolating the obtained absorbance at 590 nm in a standard curve formed by different cell densities.

2.13. Cytotoxicity assay

Cells cultured under the conditions described in point 2.2 were seeded onto 96-well tissue culture plates at 5×10^3 cells per well, and maintained under 21% pO_2 and 8% pO_2. Twenty four hours after plating the cells were treated without (control) or with the *V. baccifera* leaf extract (oxidant stimulus) for 24 h, 48 h, and 72 h. The cell viability was evaluated with the crystal violet assay [22]. Cells number was expressed as the absorbance at 590 nm, considering that absorbance is proportional to the cell density.

2.14. Statistical analysis

The statistical package SPSS 19.0 (SPSS Inc., Chicago, IL, USA) was used for data analysis. Data were expressed as mean ± standard error (SE) from at least three independent experiments. Statistical analysis of the differences of the means for one cell line at two O_2 concentrations, and for control and *V. baccifera*, was done by parametric Student's *t*-test for paired data. Comparisons between different cell lines at the same oxygen tension were performed by Student's *t*-test for unpaired data (two cell lines) or by ANOVA and *post hoc* group comparisons (three cell lines). Differences between means were considered statistically significant if $P < 0.05$. The IC_{50} (concentration that inhibits cell growth by 50%) was derived from the semi-log dose-response curve. The data were adjusted by non-linear regression ($R^2 \geq 0.99$) using GraphPad Prism 4 for Windows (San Diego, CA, USA).

3. Results

3.1. Influence of pO_2 on hepatocarcinoma features

3.1.1. Cell growth

The human HepG2, Huh7 and Hep3B hepatoma cell lines were cultured under 21% O_2 and 8% O_2, as described in Materials and Methods. Cell growth rate was determined in terms of the time required for doubling the number of cells during the exponential phase.

Results indicate that Hep3B showed the highest proliferation rate independently of the pO_2 (Table 1), whereas Huh7 had the lowest growth rate at both pO_2. Cells did not exhibit any statistically significant change of the proliferation rate depending on the oxygen tension.

3.1.2. Intracellular ROS and mitochondrial O_2^-

Intracellular ROS and mitochondrial O_2^- levels were measured by flow cytometry under both pO_2 conditions.

Huh7 showed the lowest steady-state ROS levels ($P < 0.01$), whereas the basal ROS accumulation in HepG2 was not significantly different from that in Hep3B. Reduction of pO_2 from 21% to 8% significantly increased intracellular ROS in all three cell lines (Fig. 2A). Mitochondrial O_2^- was observed in all the hepatoma cell lines, the highest levels being in Hep3B ($P < 0.05$, Fig. 2B). However, MitoSOX signals were unaffected by the culture pO_2 conditions. All in all, reduction of pO_2 induced an increase of intracellular ROS independently of the characteristics of the cell lines, while mitochondrial steady-state O_2^- levels were independent of the pO_2 in the studied oxygen range.

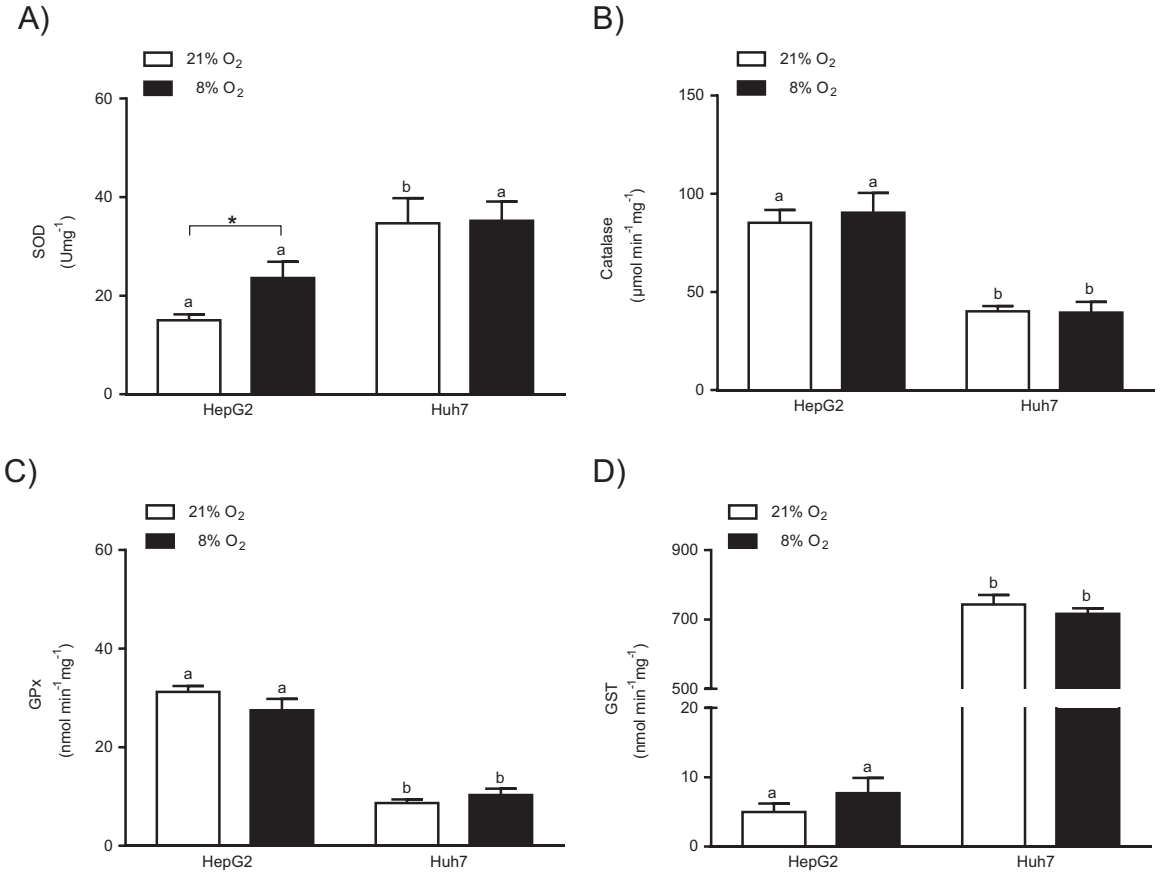

Fig. 5. Effect of pO_2 on antioxidant enzyme activities. HepG2 and Huh7 were incubated under 21% pO_2 and 8% pO_2. (A) SOD, (B) catalase, (C) GPx, and (D) GST activities were analyzed. Results are the mean+SE of 4–5 experiments. *$P < 0.05$ different between both pO_2 conditions in the same cell line. Bars with different superscript at the same pO_2 are significantly different, $^{a,b}P < 0.01$.

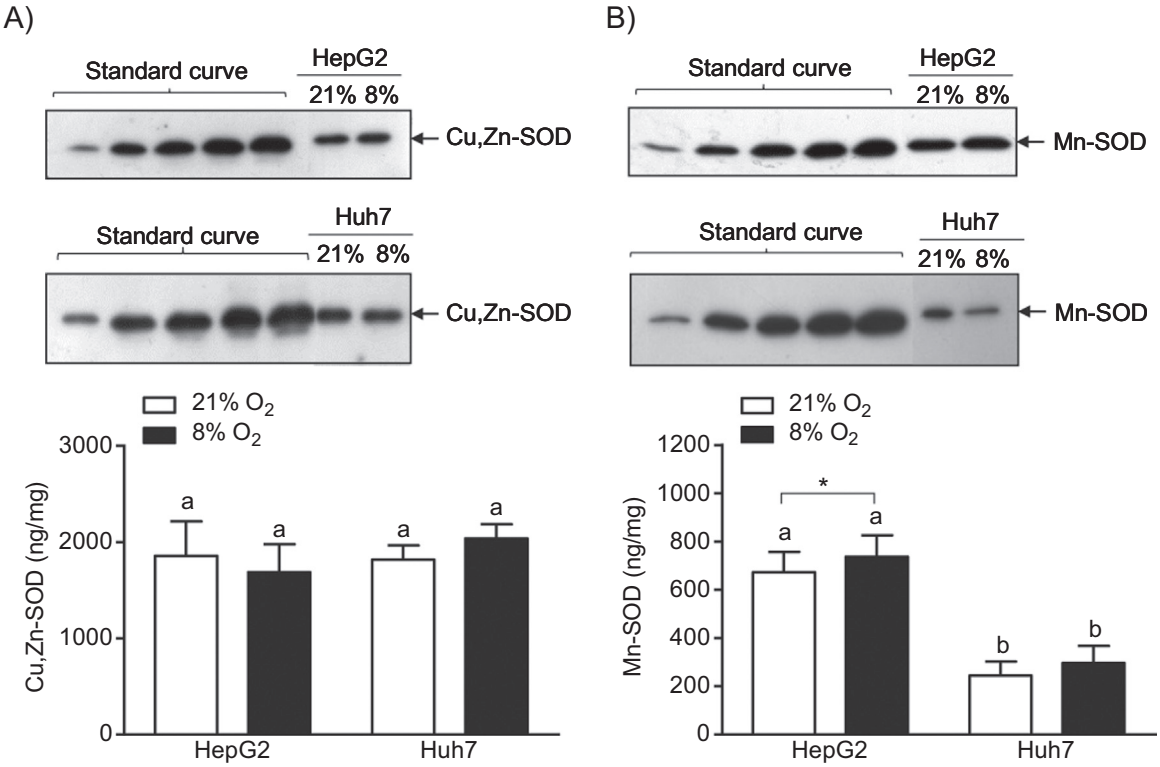

Fig. 6. Effect of pO_2 on (A) Cu,Zn-SOD and (B) Mn-SOD proteins. HepG2 and Huh7 were incubated under 21% and 8% O_2. SOD proteins were quantified by immunoblotting. A standard curve using different concentrations of recombinant protein was used to determine the absolute amount of SODs. Results are the mean+SE of 3–4 experiments. *$P < 0.05$, different between both pO_2 conditions in the same cell line. Bars with different superscript at the same pO_2 are significantly different, $^{a,b}P < 0.001$.

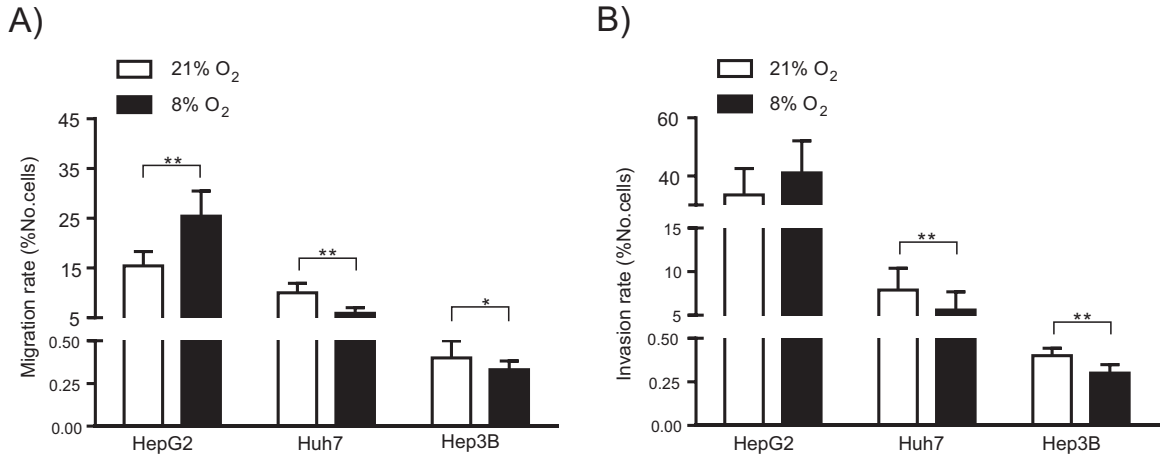

Fig. 7. Effect of pO_2 on (A) migration and (B) invasion rates in hepatoma cell lines. Cells were incubated under 21% and 8% O_2. Migration rates (number of migrated cells with respect to seeded cells) under both pO_2 are represented. Results are the mean + SE of 8–13 experiments. *P < 0.05, **P < 0.01.

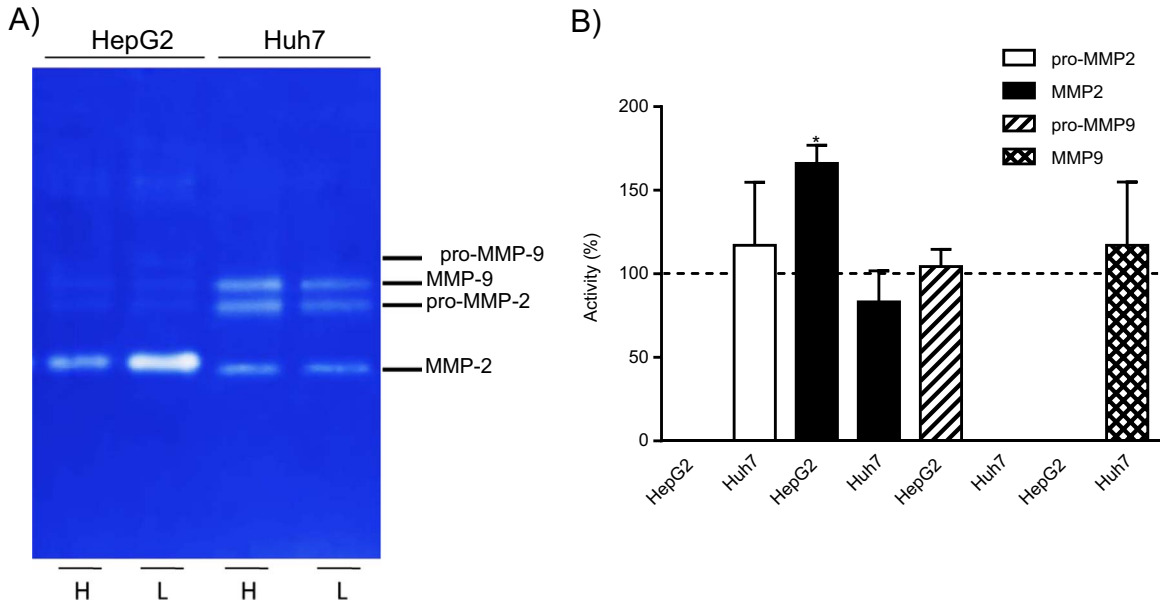

Fig. 8. Effect of pO_2 on MMPs secretion in HepG2 and Huh7 cell lines. (A) Cell conditioned medium gelatin zymography and (B) analysis of zymography results. A) Lanes correspond to HepG2 and HuH7 incubated at (H) high pO_2 (21%) and (L) low pO_2 (8%). B) Data are represented as percentage of the proteins activities at 8% O_2 compared to 21% O_2. Bars correspond to mean+SE. *P < 0.05.

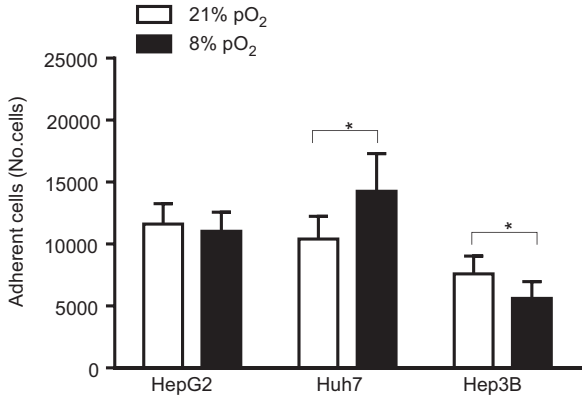

Fig. 9. Effect of pO_2 on adhesion in hepatoma cell lines. Cells grown under 21% pO_2 and 8% pO_2 were seeded (20,000 cells/well) onto 96-well plates and further incubated for 1 h. Results are the mean+SE of 4–8 experiments. *P < 0.05.

3.1.3. Glutathione

GSH has a key role in the intracellular redox homeostasis; thereby the effect of pO_2 on the intracellular glutathione levels was investigated.

A decrease in the pO_2 from 21% to 8% was associated with a significant depletion by 45% (P < 0.05) of the intracellular levels of GSH in HepG2 cells (Fig. 3). It is worth mentioning that GSH levels were detected at similar levels in all hepatoma cell lines.

3.1.4. Immunodetection of p66, p52 and p46 Shc isoforms

Due to the fact that the Shc adaptor protein mediates cell signaling, and p66 Shc is specifically implicated in regulating the intracellular level of ROS, we evaluated the effect of oxygen tension on Shc isoforms.

As can be seen in Fig. 4, Huh7 showed higher expression levels of Shc isoforms than HepG2 cells (P < 0.05), independently of the oxygen concentration. Moreover, the p66 Shc contribution to the total Shc proteins was higher in Huh7 than in HepG2 at both pO_2 (Fig. 4B). Oxygen modified the expression of Shc only in p53-wild-type HepG2 cells, the lower pO_2 (8%) up-regulating all three Shc isoforms (Fig. 4C).

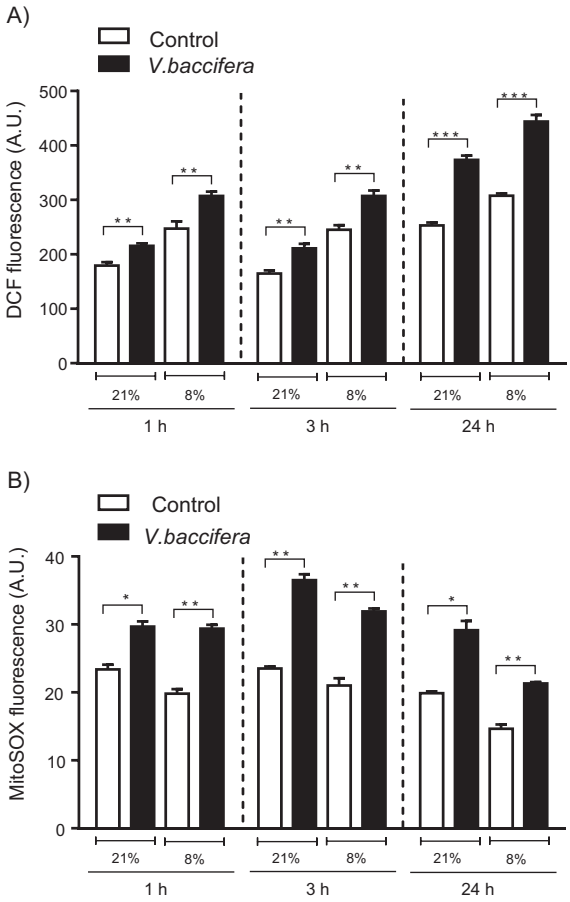

Fig. 10. Effect of *V. baccifera* on A) intracellular ROS and B) mitochondrial O_2^- levels in HepG2 cells cultured under 21% O_2 **and 8% O_2**. Cells cultured under 21% and 8% O_2 were incubated without (control) and with *V. baccifera* (75 μg/ml) for the indicated times. Arbitrary units of DCF and MitoSOX fluorescence are represented. Results are the mean+SE of 3–6 experiments. *P < 0.05, **P < 0.01, ***P < 0.001.

3.1.5. Antioxidant enzyme activities

The basal antioxidant activities of SOD, catalase, GPx, and GST in HepG2 and Huh7 were measured by spectrophotometric assays.

As can be seen in Fig. 5, SOD activity could be clearly detected in both cell lines (2-fold higher in Huh7 than in HepG2). Reduction of pO_2 from 21% to 8% significantly increased SOD activity in HepG2 ($P < 0.05$). Catalase activity varied depending on the cell line, the highest activity being observed in HepG2 (near 2-fold higher than in Huh7). However, the activity remained constant, independently of the O_2 concentration (Fig. 5B). Regarding GPx, HepG2 showed the highest activity (3.5-fold higher than that found in Huh7). The decrease in pO_2 from 21% to 8% did not have any effect on GPx activities (Fig. 5C). Concerning GST, it is interesting to note that the enzyme activity was scarcely detected under the assay limits in HepG2 cells (200–300 μg of protein used). By contrast, Huh7 exhibited elevated GST activity. The O_2 concentration did not have any effect on GST activity (Fig. 5D).

3.1.6. Quantification of Cu,Zn-SOD and Mn-SOD proteins

In view of the results on antioxidant enzymes and the significant differences found for SOD activity, we decided to study the expression of SOD isoforms by immunoblot. Human recombinant SOD protein was used to derive a standard curve and obtain absolute amounts of Cu,Zn-SOD and Mn-SOD proteins in the cell extracts.

The cytosolic isoform (Cu,Zn-SOD) was almost three-fold higher expressed than mitochondrial SOD (Mn-SOD) in HepG2 cells, and seven-fold higher in Huh7 (Fig. 6). The cytosolic isoforms were similarly expressed in both cell lines, and oxygen tension did not affect their expression (Fig. 6A). The amount of the mitochondrial SOD isoform in Huh7 was approximately 1/3 that in HepG2. The low pO_2 was associated with increased expression of Mn-SOD in HepG2 cells (Fig. 6B).

3.1.7. Cell migration and invasion

The role of ROS in triggering signaling pathways for cell migration has been well established. Through a series of cellular events, including cytoskeletal remodelling, cells are able to detach from the primary tumor and metastasize to distant sites [9]. To study the influence of oxygen on cell migration and invasion, transwell assay precoated without and with fibronectin was performed, respectively.

Independently of the pO_2 conditions, the highest migration rate was found in HepG2, and the lowest in Hep3B ($P < 0.001$). The reduction of pO_2 from 21% to 8% affected the migration capacity of the studied cells differently. Thus, the migration rate decreased in Huh7 and Hep3B, while HepG2 showed a higher migration capacity under 8% pO_2 (Fig. 7A).

Regarding the invasion transwell assay, the highest invasion rate was also found in HepG2, and the lowest in Hep3B ($P < 0.001$). The influence of the oxygen tension on invasion showed a pattern similar to that found for the migration capacity; thus, 8% pO_2 was associated with a higher, although not significant, invasion rate in HepG2, while in Huh7 and Hep3B, the invasion rate was significantly lower (Fig. 7B).

3.1.8. MMP activity

During invasion, proteolytic enzymes capable of degrading the extracellular matrix are secreted, so that the cells can migrate to new sites. The matrix metalloproteinases (MMP) are among these proteins with catalytic activity. Inactive pro-MMPs are secreted by tumor cells, and are activated upon cleavage of the pro-peptide domain by serine proteases. ROS can also activate MMP by oxidation.

Results on secretion and activation of MMPs can be seen in Fig. 8. MMP-2 secretion was clearly detected in both HepG2 and Huh7 cell lines. HepG2 secreted significantly higher MMP-2 than Huh7 ($P < 0.001$). The secretion of MMP-9 and the inactive proenzymes (pro-MMP-2 and pro-MMP-9) was detected in Huh7, but hardly found in HepG2 cells. In these cells, the proteins could not be quantified.

Quantitative analysis of the data showed that MMP-2 secretion in HepG2 increased markedly at 8% oxygen tension. MMP-2 secretion by Huh7 did not change significantly depending on the pO_2, although tended to decrease at the lower oxygen tension (Fig. 8).

3.1.9. Cell adhesion

The effect of pO_2 on cell adhesion capacity was evaluated by the crystal violet stain method. Huh7 showed the highest adhesion capacity under 8% pO_2, while Hep3B showed the lowest ($P < 0.05$) (Fig. 9). Cell adhesion was differently affected by pO_2 in every one of the studied hepatoma cell lines. Thus, a low pO_2 favoured Huh7 adhesiveness, contrary to the effect in Hep3B. The HepG2 adhesion capacity did not depend on pO_2.

3.2. *Effect of pO_2 on* V. baccifera*-induced toxicity in HepG2*

In the next step, the aim was to determine whether pO_2 affected the cell response to an oxidant stimulus. In a previous work we described that the aqueous leaf extract of the Amazonian *V. baccifera* plant was cytotoxic to HepG2 cells cultured at 21% O_2 and this toxicity was suggested to be mediated by ROS [18]. We have used this system as the oxidant source. HepG2 cells were grown as indicated in Materials and Methods under 21% and 8% O_2. After that, intracellular cells were exposed to the plant extract under both pO_2 conditions and intracellular ROS, mitochondrial O_2^- and cytotoxiciy were determined.

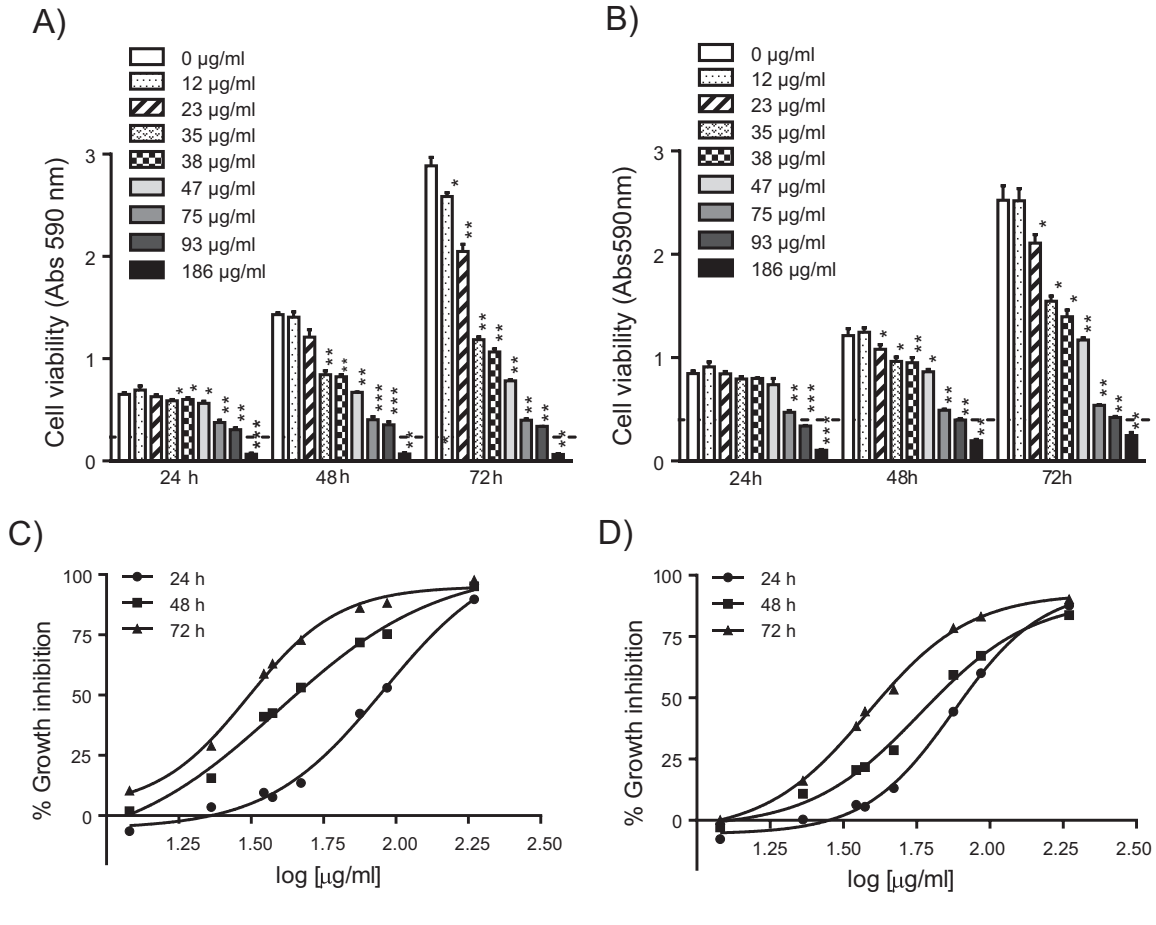

E)

	IC_{50} (µg/ml)		
	24 h	48 h	72 h
21% pO_2	87.6 ± 3.4	44.9 ± 0.8	31.2 ± 0.3
8% pO_2	81.1 ± 1.5	65.5 ± 2.4*	42.3 ± 2.1*

Fig. 11. Effect of *V. baccifera* on growth of HepG2 cells cultured under (A, C) 21% O_2 **and (B, D) 8% O_2**. (A, B) Results are the mean+SE of 3 experiments. The value of the control at time zero was 0.30 and 0.39 absorbance units at 21% and 8% pO_2, respectively, and is represented as a dashed line in the figures. *P < 0.05, **P < 0.01, ***P < 0.001 compared with control (without *V. baccifera*). (C, D) The data were fitted to dose-response curves by nonlinear regression (R^2=0.99). (E) IC_{50} (concentration that inhibits 50% of cell growth). *P < 0.05, significantly different between both O_2 concentrations.

3.2.1. Intracellular ROS and mitochondrial O_2^-

V. baccifera induced ROS accumulation from the first analyzed time, and this effect was independent on the pO_2 (Fig. 10A). In the same way, the plant extract induced increases in mitochondrial O_2^- steady-state levels; these increases were not influenced by pO_2 (Fig. 10B).

3.2.2. Cell toxicity

Cell toxicity was studied by crystal violet stain method. As is shown in Fig. 11, under atmospheric pO_2 *V. baccifera* significantly reduced cell viability in a dose- and time-dependent manner. The IC_{50} derived values showed that cell lines maintained at 8% pO_2 were more resistant to the extract than their counterparts that were maintained at 21% pO_2.

4. Discussion

Numerous physiological studies have been performed using *in vitro* models of cancer cell lines usually cultured under atmospheric O_2 concentrations. However, the physiological concentrations of O_2 in the tissues are far from these values. Oxygen can induce changes in the proteome and the genome of the neoplastic cells [32], and modify the intracellular ROS production. Knowing the drastic consequences of oxidative stress on the cell physiology, we considered it was essential to study the cellular behaviour under a more physiological pO_2 (8%), and compare the cell phenotype with that found for the same cells cultured under 21% O_2. To investigate the implication of p53 in these changes, we used human hepatoma cell lines with different p53 expressions, HepG2 (wilde type), Huh7 (mutated), and Hep3B (deleted). Our results indicated that the cell growth of HepG2, Huh7, and Hep3B was not influenced by the pO_2 in the range used. In contrast, the oxygen tension

modified the intracellular steady-state ROS levels; thus, a low pO_2 resulted in higher ROS in all the cell lines, suggesting that the ROS increase induced by low oxygen is independent of p53. Interestingly, the steady-state mitochondrial levels of O_2^- were not modified by the oxygen concentration. To this respect, early and transient increases in O_2^- in response to acute hypoxia have been described in several cell types. The superoxide production burst in the first minutes is proposed to be the cause of redox-based adaptations of the cells to hypoxia [33]. In the literature, and according to our results, it has been reported that high atmospheric O_2 concentrations are associated with reduced ROS levels and higher GSH concentrations in pulmonary cells [34]. In our system, the long-term culturing of the p53 wild-type HepG2 cell line under low O_2 (8%) for several days induced a marked depletion of the intracellular GSH content and a significantly higher expression of Shc isoforms. These effects were not found in the other two cell lines with lower or null p53 expression. The p66 Shc isoform is induced transcriptionally by p53 [35], and generates H_2O_2 by directly transferring electrons from cytochrome c to molecular oxygen [36]. As mentioned, although both HepG2 (wild-type p53) and Huh7 (mutant p53) expressed p66 Shc protein, at 8% pO_2 the expression of Shc isoforms was increased only in HepG2, agreeing that p66 Shc is a p53 downstream effector. ROS increase often leads to GSH depletion and alterations of the redox balance [37]. Similar to the results on pulmonary cells described by Kumar et al. [34], Lawrence et al. also found that long-term culturing at low oxygen partial pressure of human and mouse myeloid cell lines reduced the intracellular GSH content, compared with their counterparts that were maintained at atmospheric oxygen [11].

It has been reported that ROS are the critical signal messengers for migration through MAPK pathway [38], and adhesion [39]. In our system, the migratory and adhesiveness capacities depended on the cell line characteristics. In fact, HepG2 had the highest migration, invasion and adhesion rates. Moreover, the pO_2 modified the cell migration and secretion of active metalloproteinases. Thus, a low pO_2 increased the migration rate and secretion of MMP-2 in wild-type p53 HepG2, whereas p53 deficient cells exhibited a slower migration and a similar MMPs secretion. Interestingly, in our laboratory we have detected by immunoblotting higher p53 stabilization when HepG2 were cultured under 8% pO_2 (data not shown), these results suggesting the role of p53 in hepatocarcinoma metastatic activity.

In response to initial slight oxidative stress, cells adapt by up-regulating the expression of antioxidant enzymes, which can contribute to reduce the initial ROS accumulation. Our results also showed that low oxygen tension was associated with significant long-term changes in the antioxidant enzyme system, which was reflected in an increased SOD activity and the up-regulation of the mitochondrial Mn-SOD expression. p53 can exert opposite responses depending on the intensity and persistence of the oxidant stimulus and trigger activation of antioxidant systems [13]. The induction of MnSOD may have a role on pro-survival, progression, and invasion responses of HepG2 cells to the low oxygen concentration. This adaptation could modify the response of HepG2 cells to the *V. baccifera*-induced oxidant stress, being more resistant than the cells grown under higher pO_2.

5. Conclusions

The present study indicates that pO_2 affects the tumor characteristics of human hepatocellular carcinoma cells, suggesting that the long-term culture under low, more physiological O_2 induces antioxidant adaptations that may modify their response to a subsequent oxidant challenge. These adaptations could be mediated by p53. Data support the necessity of validating data obtained from *in vitro* studies using human cell lines cultured under atmospheric oxygen in order to draw conclusions on cancer biology and the mechanisms of action of anticancer drugs.

Acknowledgements

This work was supported by research grants from the Basque Government (Department of Education, Universities and Research, ref. IT687-13), and University of the Basque Country, UPV/EHU (CLUMBER UFI11/20 and pre-doctoral and post-doctoral grants to J.T.). We thank José Antonio López for his valuable technical assistance with cell cultures. Technical and human support provided by SGIKer (UPV/EHU, MICINN, GV/EJ, ESF) is gratefully acknowledged.

References

[1] A.J. Brooks, J. Eastwood, I.J. Beckingham, K.J. Girling, Liver tissue partial pressure of oxygen and carbon dioxide during partial hepatectomy, Br. J. Anaesth. 5 (2004) 735–737.
[2] A. Carreau, B. El Hafny-Rahbi, A. Matejuk, C. Grillon, C. Kieda, Why is the partial oxygen pressure of human tissues a crucial parameter? Small molecules and hypoxia, J. Cell. Mol. Med. 6 (2011) 1239–1253.
[3] L. Jagannathan, S. Cuddapah, M. Costa, Oxidative stress under ambient and physiological oxygen tension in tissue culture, Curr. Pharmacol. Rep. 2 (2016) 64–72.
[4] J.K. Saggar, M. Yu, Q. Tan, I.F. Tannock, The tumor microenvironment and strategies to improve drug distribution, Front. Oncol. (2013) 154.
[5] J.F. Turrens, B.A. Freeman, J.G. Levitt, J.D. Crapo, The effect of hyperoxia on superoxide production by lung submitochondrial particles, Arch. Biochem. Biophys. 2 (1982) 401–410.
[6] B. Halliwell, Oxidative stress in cell culture: an under-appreciated problem?, FEBS Lett. 1–3 (2003) 3–6.
[7] B. Halliwell, Cell culture, oxidative stress, and antioxidants: avoiding pitfalls, Biomed. J. 3 (2014) 99–105.
[8] C. Lennicke, J. Rahn, R. Lichtenfels, L.A. Wessjohann, B. Seliger, Hydrogen peroxide - production, fate and role in redox signaling of tumor cells, Cell. Commun. Signal. (2015) 39–015-0118-6.
[9] L. Tochhawng, S. Deng, S. Pervaiz, C.T. Yap, Redox regulation of cancer cell migration and invasion, Mitochondrion 3 (2013) 246–253.
[10] A. Carreau, B. El Hafny-Rahbi, A. Matejuk, C. Grillon, C. Kieda, Why is the partial oxygen pressure of human tissues a crucial parameter? Small molecules and hypoxia, J. Cell. Mol. Med. 6 (2011) 1239–1253.
[11] D.A. Lawrence, R.J. Colinas, A.C. Walsh, Influence of oxygen partial pressure on human and mouse myeloid cell line characteristics, Fundam. Appl. Toxicol. 2 (1996) 287–293.
[12] A.V. Vaseva, U.M. Moll, The mitochondrial p53 pathway, Biochim. Biophys. Acta 5 (2009) 414–420.
[13] G. Pani, T. Galeotti, Role of MnSOD and p66shc in mitochondrial response to p53, Antioxid. Redox Signal. 6 (2011) 1715–1727.
[14] A. Maillet, S. Pervaiz, Redox regulation of p53, redox effectors regulated by p53: a subtle balance, Antioxid. Redox Signal. 11 (2012) 1285–1294.
[15] S. Perrini, F. Tortosa, A. Natalicchio, C. Pacelli, A. Cignarelli, V.O. Palmieri, C. Cacciopoli, F. De Stefano, S. Porro, A. Leonardini, F. Giorgino, The p66Shc protein controls redox signaling and oxidation-dependent DNA damage in human liver cells, Am. J. Physiol. Gastrointest. Liver Physiol. 10 (2015) G826–G840.
[16] M. Giorgio, E. Migliaccio, F. Orsini, D. Paolucci, M. Moroni, C. Contursi, G. Pelliccia, L. Luzi, S. Minucci, M. Marcaccio, P. Pinton, R. Rizzuto, P. Bernardi, F. Paolucci, P.G. Pelicci, Electron transfer between cytochrome C and p66Shc generates reactive oxygen species that trigger mitochondrial apoptosis, Cell 2 (2005) 221–233.
[17] P. Pinton, A. Rimessi, S. Marchi, F. Orsini, E. Migliaccio, M. Giorgio, C. Contursi, S. Minucci, F. Mantovani, M.R. Wieckowski, G. Del Sal, P.G. Pelicci, R. Rizzuto, Protein kinase C beta and prolyl isomerase 1 regulate mitochondrial effects of the life-span determinant p66Shc, Science 5812 (2007) 659–663.
[18] L.J. Lizcano, M. Siles, J. Trepiana, M.L. Hernandez, R. Navarro, M.B. Ruiz-Larrea, J.I. Ruiz-Sanz, Piper and Vismia species from Colombian Amazonia differentially affect cell proliferation of hepatocarcinoma cells, Nutrients 1 (2014) 179–195.
[19] Y. Lin, C.Y. Shi, B. Li, B.H. Soo, S. Mohammed-Ali, A. Wee, C.J. Oon, P.O. Mack, S.H. Chan, Tumour suppressor p53 and Rb genes in human hepatocellular carcinoma, Ann. Acad. Med. Singap. 1 (1996) 22–30.
[20] I.C. Hsu, T. Tokiwa, W. Bennett, R.A. Metcalf, J.A. Welsh, T. Sun, C.C. Harris, p53 gene mutation and integrated hepatitis B viral DNA sequences in human liver cancer cell lines, Carcinogenesis 5 (1993) 987–992.
[21] L.J. Lizcano, F. Bakkali, M. Begoña Ruiz-Larrea, J. Ignacio Ruiz-Sanz, Antioxidant activity and polyphenol content of aqueous extracts from Colombian Amazonian plants with medicinal use, Food Chem. 4 (2010) 1566–1570.
[22] R.J. Gillies, N. Didier, M. Denton, Determination of cell number in monolayer cultures, Anal. Biochem. 1 (1986) 109–113.
[23] I. Rahman, A. Kode, S.K. Biswas, Assay for quantitative determination of glutathione and glutathione disulfide levels using enzymatic recycling method, Nat. Protoc. 6 (2006) 3159–3165.
[24] U.K. Laemmli, Cleavage of structural proteins during the assembly of the head of bacteriophage T4, Nature 5259 (1970) 680–685.
[25] M.M. Bradford, A rapid and sensitive method for the quantitation of microgram quantities of protein utilizing the principle of protein-dye binding, Anal. Biochem. (1976) 248–254.

[26] J.Y. Zhou, P. Prognon, Raw material enzymatic activity determination: a specific case for validation and comparison of analytical methods–the example of superoxide dismutase (SOD), J. Pharm. Biomed. Anal. 5 (2006) 1143–1148.
[27] J.M. McCord, I. Fridovich, Superoxide dismutase. An enzymic function for erythrocuprein (hemocuprein), J. Biol. Chem. 22 (1969) 6049–6055.
[28] H. Aebi, Catalase in vitro, Methods Enzymol. (1984) 121–126.
[29] L. Flohe, W.A. Gunzler, Assays of glutathione peroxidase, Methods Enzymol. (1984) 114–121.
[30] W.H. Habig, W.B. Jakoby, Assays for differentiation of glutathione S-transferases, Methods Enzymol. (1981) 398–405.
[31] D.E. Kleiner, W.G. Stetler-Stevenson, Quantitative zymography: detection of picogram quantities of gelatinases, Anal. Biochem. 2 (1994) 325–329.
[32] M. Hockel, P. Vaupel, Tumor hypoxia: definitions and current clinical, biologic, and molecular aspects, J. Natl. Cancer Inst. 4 (2001) 266–276.
[33] P. Hernansanz-Agustín, A. Izquierdo-Álvarez, F.,J. Sánchez-Gómez, E. Ramos, T. Villa-Piña, S. Lamas, A. Bogdanova, A. Martínez-Ruiz, Acute hypoxia produces a superoxide burst in cells, Free Radic. Biol. Med. 71 (2014) 146–156.
[34] A. Kumar, L.A. Dailey, M. Swedrowska, R. Siow, G.E. Mann, G. Vizcay-Barrena, M. Arno, I.S. Mudway, B. Forbes, Quantifying the magnitude of the oxygen artefact inherent in culturing airway cells under atmospheric oxygen versus physiological levels, FEBS Lett. 2 (2016) 258–269.
[35] M. Trinei, M. Giorgio, A. Cicalese, S. Barozzi, A. Ventura, E. Migliaccio, E. Milia, I.M. Padura, V.A. Raker, M. Maccarana, P.G. Pelicci, A p53-p66Shc signalling pathway controls intracellular redox status, levels of oxidation-damaged DNA and oxidative stress-induced apoptosis, Oncogene 24 (2002) 3872–3878.
[36] M. Giorgio, M. Trinei, E. Migliaccio, P.G. Pelicci, Hydrogen peroxide: a metabolic by-product or a common mediator of ageing signals, Nat. Rev. Mol. Cell Biol. 9 (2007) 722–728.
[37] G. Wu, Y.Z. Fang, S. Yang, J.R. Lupton, N.D. Turner, Glutathione metabolism and its implications for health, J. Nutr. 3 (2004) 489–492.
[38] W.S. Wu, J.R. Wu, C.T. Hu, Signal cross talks for sustained MAPK activation and cell migration: the potential role of reactive oxygen species, Cancer Metastas-. Rev. 2 (2008) 303–314.
[39] P. Chiarugi, Reactive oxygen species as mediators of cell adhesion, Ital. J. Biochem. 1 (2003) 28–32.